Pergamon

SCIENCE DIRECT®

Tetrahedron: *Asymmetry* 14 (2003) 3117–3122

TETRAHEDRON: *ASYMMETRY*

Determination of the rotational barrier of a chiral biphenyl: Comparison of theoretical and experimental data

Francesca Ceccacci,[a] Giovanna Mancini,[b] Paolo Mencarelli[a,*] and Claudio Villani[c]

[a]*Dipartimento di Chimica, Università degli Studi di Roma "La Sapienza", P. le A. Moro 5, I-00185 Roma, Italy*
[b]*CNR, IMC c/o Dipartimento di Chimica, Università degli Studi di Roma "La Sapienza", P. le A. Moro 5, I-00185 Roma, Italy*
[c]*Dipartimento di Studi di Chimica e Tecnologia delle Sostanze Biologicamente Attive, Università degli Studi di Roma "La Sapienza", P. le A. Moro 5, I-00185 Roma, Italy*

Received 7 May 2003; accepted 14 July 2003

Abstract—The rotational barrier of chiral 2-carboxy-2′-methoxy-6-nitrobiphenyl has been evaluated both by density functional calculations, at the B3LYP/6-31G(d) and B3LYP/6-311+G(d,p) levels of theory, and by HF and post HF MP2 calculations at the 6-31G(d) level of theory. The DFT computed data, which seemed almost independent of the basis set used, are in good agreement with the values obtained from dynamic HPLC enantiomerization experiments and from the racemization rate constant of one of the enantiomers obtained by CD. The HF model seems to overestimate the barrier whereas the MP2 calculations confirm the DFT results.

1. Introduction

The study of the non-covalent interactions responsible for chiral recognition is of crucial importance from many perspectives. It may help to address the design of more appropriate catalysts for enantioselective or diastereoselective reactions; it may also shed some light on chiral recognition in metabolic pathways and may help to clarify possible amplification mechanisms that lead to the present homochirality of biomolecules.

The use of atropoisomeric compounds in a chiral recognition investigation[1–4] is very useful, not only because it avoids expensive and time demanding enantioseparations, but also because it allows us to quite easily reveal a very small enantiomeric excess by using the proper technique and compound. In fact the deracemization of the racemic mixture of dichroic atropoisomeric compounds, induced by diastereomeric interactions, can easily be detected whereas the corresponding difference between the association constants of the enantiomers to the chiral auxiliary may not be detectable.

In the choice of the atropoisomeric compound, a fundamental point is the estimation of the rotational barrier, which must be such as to allow interconversion of the enantiomers at the investigation temperature. The kinetic determination of the racemization rate constant, following the change of optical activity as a function of time, requires the separation of the enantiomers and therefore it is not always an easy task. In the case of a chromatographic approach it is, in fact, necessary to identify a proper chiral phase and the appropriate temperature in order to resolve successfully the racemate. Moreover if the rotational barrier is low and the racemization is consequently fast at ambient temperature, operating at low temperatures may be somewhat troublesome. The indirect experimental determination of the enantiomerization[†] rate constant by other methods such as dynamic HPLC or dynamic NMR can also be difficult. In fact, the same difficulties involved in the chromatographic resolution of the racemate have to be faced in the use of dynamic HPLC. On the other hand the possibility of determining the enantiomerization rate constant by dynamic NMR depends on the presence of diastereotopic or diastereomeric signals and requires an opportune chemical shift difference between

* Corresponding author. Tel.: +39-0649913697; fax: +39-06490631; e-mail: paolo.mencarelli@uniroma1.it

† Racemization is the conversion of an enantiomerically pure compound or of an enantiomerically enriched mixture into a racemate:
(+)-A→(±)-A
Enantiomerization is the conversion of one enantiomer into the other:
(+)-A→(−)-A
The overall racemization rate costant, k_{rac}, is linked to the enantiomerization rate costant, k_1, by the relation $k_{rac}=2k_1$.

0957-4166/$ - see front matter © 2003 Elsevier Ltd. All rights reserved.
doi:10.1016/S0957-4166(03)00544-5

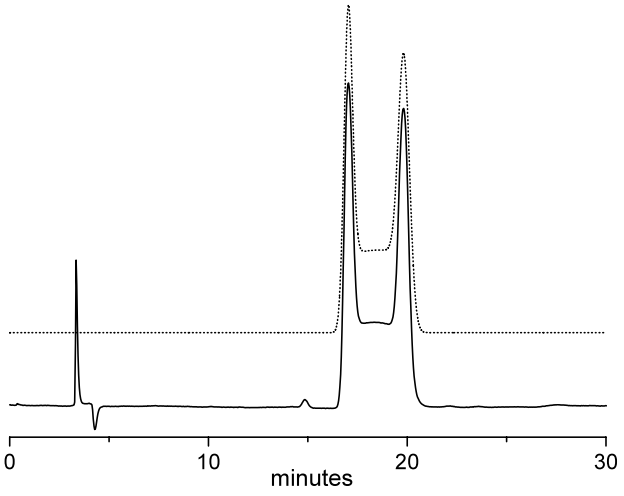

Figure 1. Experimental (solid) and simulated (dot, vertically shifted) chromatograms of **2** on a chiral stationary phase. Experimental: Chiralpak AD 250×4.6 mm i.d. column; eluent hexane/isopropanol 95/5+0.1% trifluoroacetic acid; temperature 297 K, flow rate 1.0 ml/min; UV @ 254 nm. Simulated: $N_1=5000$; $N_2=4200$; $k_m=0.1$ min^{-1}.

the signals. As a consequence, the theoretical estimation of the rotational barrier could be an appropriate method and, more often than not, the only choice available.

In the framework of our investigation on chiral recognition in self-assemblies,[1–3] we have been using chiral biphenylic derivatives in order to point out by deracemization even small recognition events, these compounds being characterized by high molar ellipticity. In our work a reliable theoretical determination of the rotational barrier of biphenylic derivatives is a major requirement: It can in fact address the choice of the right compound, avoiding time demanding preparation of compounds characterized by a too high rotational barrier.

In our deracemization experiments we have been using 2-carboxy-2′-dodecyloxy-6-nitrobiphenyl **1** and we know that its rotational barrier allows interconversion of the enantiomers at room temperature.[2,5] Herein we report studies on a simpler homologue of **1**, i.e. 2-carboxy-2′-methoxy-6-nitrobiphenyl **2**, which, in our opinion, is the correct candidate for a study that, comparing experimental and theoretical results, might allow us to evaluate the reliability of theoretical calculations.

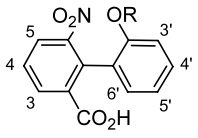

1 R= $C_{12}H_{25}$
2 R= CH_3

The racemization of **2** has already been studied by polarimetry during the 1930s and a rotational barrier of approximately 20 kcal/mol was reported.[6] However, from the literature it was not evident how the authors elaborated the raw kinetic data. Therefore, it seemed appropriate to experimentally re-evaluate the barrier both by dynamic HPLC and, after separation of the two enantiomers, by direct kinetic determination of the racemization rate constant of one of the enantiomers by CD. At the same time, theoretical calculations based on the density functional theory provided us with a computed value for the rotational barrier to be compared with the experimental ones.

2. Experimental results

2.1. Dynamic HPLC

The enantiomers of **2** were resolved by HPLC on an amylose carbamate chiral stationary phase. When the column temperature was set in the 288–298 K range, two well resolved peaks were observed in the chromatograms, with a plateau-like region clearly visible between the peaks. The presence of such band deformations is indicative of on-column enantiomer interconversion, occurring at a rate similar to that of the separation process.[7] The dynamic chromatographic profiles changed in a manner that is dependent on both the eluent flow rate and column temperature. At a constant flow rate (1.0 ml/min on the analytical column) the area under the plateau progressively diminished as the column temperature was lowered and eventually disappeared around 275 K, leaving two baseline resolved peaks as a result of slow interconversion on the time scale of the separation process. At a constant column temperature (297 K), the extent of interconversion diminished as the eluent flow rate was increased, although the effects on the peaks deformation were much less pronounced than those observed in response to the changes in the column temperature. Such dynamic deformations of the experimental chromatograms were exploited to extract kinetic data pertinent to the enantiomerization process occurring during chromatography. Computer simulations[8] of exchange-deformed elution profiles, obtained at 297 K and using an eluent flow rate of 1.0 ml/min, gave the apparent rate constants for the on-column stereomutation process $k_a^{\rightarrow}=0.035$ min^{-1} and $k_a^{\leftarrow}=0.030$ min^{-1}, where $k_a^{\rightarrow}$ is the apparent kinetic constant for the conversion of the first into the second eluted enantiomer and $k_a^{\leftarrow}$ is the kinetic constant for the backward process (see Fig. 1). The apparent rate constants $k_a^{\rightarrow}$ and $k_a^{\leftarrow}$ thus obtained are averaged values for the interconversion occurring in the mobile ($k_m^{\rightarrow}=k_m^{\leftarrow}$) and in the stationary ($k_s^{\rightarrow}\neq k_s^{\leftarrow}$) phases. Although the values of the apparent rate constants obtained by simulation may differ in principle from k_m, in practice they are usually very close to those determined by independent measurements in solution and can be used to determine the energy barrier for the dynamic process.

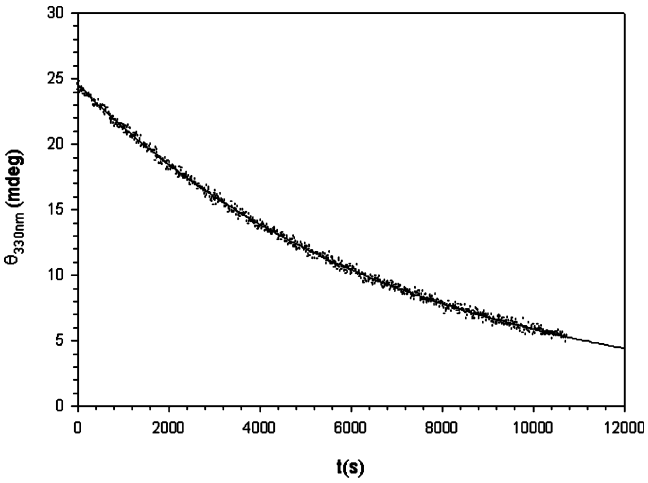

Figure 2. CD exponential decay curve at $\lambda=330$ nm and at $T=282$ K relative to the racemization process of one enantiomer of **2**.

Using the apparent rate constants $k_a^{\rightarrow}$ and $k_a^{\leftarrow}$ determined by simulation, we found $\Delta G_{297}^{\#\rightarrow}=21.8\pm0.2$ kcal/mol and $\Delta G_{297}^{\#\leftarrow}=21.9\pm0.2$ kcal/mol, in close agreement with the barrier found by thermal racemization in free solution (see below).

2.2. Kinetic studies

After resolution of racemic 2-carboxy-2′-methoxy-6-nitrobiphenyl **2** by low temperature HPLC on a chiral stationary phase, the racemization kinetic of the pure enantiomer in a mixed solvent (methanol/water = 5/1+0.1% TFA) at $T=282$ K was followed by CD at $\lambda=330$ nm (Fig. 2).

The racemization of the enantiomerically pure biphenylic derivative is a first order process in which the rate constants for the forward and the reverse path are numerically identical, with each individual path being an enantiomerization process which we cannot observe in isolation. In the case of a racemization process, the general kinetic equation (1) for a first order reversible reaction,

$$\ln\left\{\frac{[A]_t-[A]_e}{[A]_0-[A]_e}\right\}=(k_1+k_{-1})t \qquad (1)$$

where $[A]_0$, $[A]_t$ and $[A]_e$ are the concentrations at time $t=0$, at time t and at the equilibrium, respectively, and, k_1 and k_{-1} are the enantiomerization rate constants for the forward and the reverse process, can be rearranged into equation (2):[9]

$$\ln\left\{\frac{[\theta]_t}{[\theta]_0}\right\}=-2k_1t \qquad (2)$$

with θ_0 being the ellipticity at $t=0$, θ_t the ellipticity at t and $k_1=k_{-1}$.

The experimental decay curve obtained from the CD study was fitted by a non-linear least squares analysis to an exponential function (Fig. 2) and from the obtained value $k_1=(7.14\pm0.03)\times10^{-5}$ s^{-1} the activation energy for the enantiomerization process, $\Delta G^{\#}=21.8\pm0.1$ kcal/mol, was calculated by the Eyring equation.

3. Computational model

Since it is known that the electron correlation should be taken into account when dealing with rotational barriers in biphenyls,[10] in order to keep the computational effort within reasonable limits, we choose the density functional theory (DFT) approach as a theoretical method. It is known that this method may achieve a greater accuracy than the Hartree–Fock (HF) theory, at a modest increase of cost. The DFT approach overcomes the major limitation of the HF theory, i.e. the neglect of electron correlation, by including some of the electron correlation effects. Its results may be compared to the post HF MP2 method.[11] It has recently been shown that DFT calculations provide the torsional barriers of biphenyls in good accord with the experimental values,[12] whereas the HF approach overestimates them.[10]

All the calculations were carried out by using the Gaussian 98 package.[13] The DFT approach was used with the Becke's three-parameter functional and with the correlation functional of Lee, Yang, and Parr (B3LYP). In order to check the effect of the basis set, the calculations were carried out at two levels of theory: at first, the 6-31G(d) basis set, a split valence basis set supplemented with polarization d-functions on heavy atoms was used and subsequently all the stationary points found were reoptimized with the 6-311+G(d,p) basis set, a triple zeta basis set, plus diffuse functions added to heavy atoms and with polarization p-functions on hydrogen and 2-d functions on heavy atoms. The ground state structure and the transition states for the enantiomerization of **2** were fully optimized, and each stationary point found was characterized by a frequency calculation. For the structures featuring one imaginary frequency and therefore found to be a saddle point, the normal mode corresponding to the imaginary frequency, was animated by using the visualization program Molden.[14] In this way it was verified that the displacements that compose the mode lead to the two enantiomeric structures. The two rotational barriers were obtained as the difference between the total energies, including the zero-point and thermal corrections, of the minimum and the two transition states. In order to check the performance of this model for our type of biphenyl, the same calculations, with the same procedure stated above, were also carried out at the HF/6-31G(d) level of theory. To evaluate the effect of the inclusion of the electron correlation, single point calculations at the MP2/6-31G(d) level of theory, on the structures fully optimized at the HF/6-31G(d) level of theory, were also carried out.

Table 1. Total energies and relative energies obtained from the DFT calculations

	B3LYP/6-31G(d)		B3LYP/6-311+G(d,p)	
	E^a (a.u.)	ΔE (kcal/mol)	E^a (a.u.)	ΔE (kcal/mol)
Minimum	–970.630533	0	–970.909614	0
(*Z*)-TS	–970.596776	21.18	–970.875889	21.16
(*E*)-TS	–970.594271	22.75	–970.873091	22.92

[a] Zero-point and thermal corrections (at 298.15 K) included.

Table 2. Total energies and relative energies obtained from the HF and MP2 calculations

	HF/6-31G(d)		MP2/6-31G(d)//HF/6-31G(d)	
	E^a (a.u.)	ΔE (kcal/mol)	E (a.u.)	ΔE (kcal/mol)
Minimum	–964.931126	0	–968.034738	0
(*Z*)-TS	–964.891825	24.66	–968.000658	21.39
(*E*)-TS	–964.889319	26.23	–967.998831	22.53

[a] Zero-point and thermal corrections (at 298.15 K) included.

4. Computational results

The results obtained for the energies are reported in Table 1 for the DFT B3LYP/6-31G(d), and B3LYP/6-311+G(d,p) calculations, and in Table 2 for the HF/6-31G(d) and the MP2/6-31G(d)//HF-6-31G(d) calculations. In Figure 3, the two enantiomerization pathways are depicted. Only one minimum energy structure was found for the non-planar ground state of **2** together with two transition states: (*Z*)-TS and (*E*)-TS. For the DFT calculations, at both levels of theory, in the minimum structure of **2**, the dihedral angle C2–C1–C1′–C2′ between the two phenyl rings was found to be very close to 90° (−83.5, −82.9). The (*Z*)-transition state was found to be more stable than the (*E*) one at both levels of theory. Therefore, being the barrier relative to the (*Z*)-transition state the lowest, this is the one to compare with the experimental data. Both energy barriers seem almost independent on basis set. An interesting feature was found in the

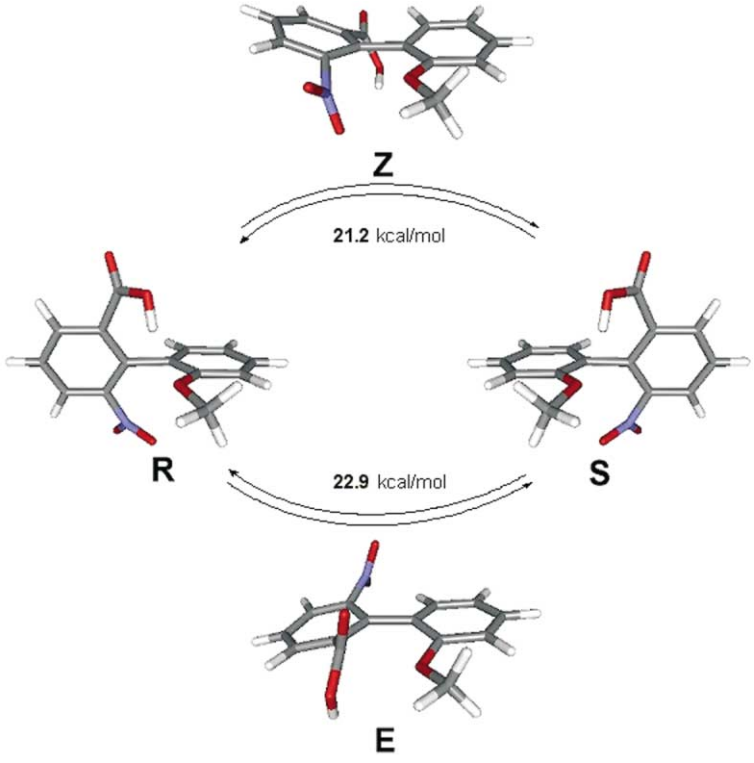

Figure 3. B3LYP/6-311+G(d,p) optimized structures for the ground state and (*E*) and (*Z*)-transition states of the enantiomerization of **2**. The two energy barriers are also reported (see text for details).

ground state structure of **2**: the short distance (1.84–1.85 Å) between the hydrogen atom of the carboxylic group and the oxygen atom of the methoxy group strongly suggests the existence of an intramolecular hydrogen bond. Such a hydrogen bond is lost in both (*Z*)- and (*E*)-transition states where the H···O distances are 4.52–4.61 Å and 2.82–2.83 Å, respectively.

The results obtained from the HF/6-31G(d) calculations are similar to those obtained from the DFT model: the (*Z*)-transition state was found to be more stable than the (*E*) one and the dihedral angle C2–C1–C1′–C2′ between the two phenyl rings in the minimum structure of **2** was found to be −87.9°. Also the existence of an intramolecular hydrogen bond between the hydrogen atom of the carboxylic group and the oxygen atom of the methoxy group was confirmed by the short distance found (2.04 Å).

5. Discussion

In Table 3 the experimental and computational values obtained in this work for the rotational barrier of **2** are reported.

The two values obtained by dynamic HPLC and circular dichroism are coincident within the experimental errors, even if they were obtained in two different solvent mixtures and at two different temperatures. As stated above, the two values obtained from the DFT calculations are also almost coincident and therefore the rotational barrier seems independent on the basis set used for the calculation. The computational value, 21.2 kcal/mol, is in good agreement with the two experimental ones, 21.8–21.9 kcal/mol. By way of contrast, the value obtained at the HF/6-31G(d) level of theory, 24.66 kcal/mol, is substantially higher than the experimental values, with this finding in accordance with the results obtained for the polychlorobiphenyls.[10] The result obtained for the barrier from the MP2/6-31G(d)//HF/6-31G(d) single point calculations, 21.39 kcal/mol, demonstrates the crucial effect of the electron correlation on the barrier and confirms the good performances of the DFT model.

Finally, it should be noted that the experimental rotational barriers are free activation energies, whereas the computed ones, being obtained as differences of the total energies corrected for the zero-point and thermal corrections differences (at 298.15 K), do not contain the entropic contributions to the barrier. A negative value for the ΔS of activation is expected because in both transition states, due to their quasi-planar structure, the rotation of the NO_2, CH_3O and COOH groups can be somewhat restricted. However, the above mentioned intramolecular hydrogen bond suggests that also in the ground state the rotation of the CH_3O and COOH groups is not completely free and so, a small negative value for the ΔS of activation should be expected. This hypothesis is in accordance with the observation that the two experimental values for the free energy of activation are practically coincident, even if the measurements were carried out at two different temperatures.

In conclusion the results of this work indicate that the rotational barriers of this type of biphenyl can be reliably predicted by theoretical DFT calculations even at the B3LYP/6-31G(d) level of theory, whereas the HF model seems to overestimate them. The results are comparable to those obtained with the post HF MP2 model, but are less expensive in terms of computational time. As previously stated, since the computed value for the rotational barrier does not contain the entropic contributions, it can be considered the lower limit for such a barrier and thus provides an upper limit for the enantiomerization rate constant. Consequently it can be very helpful in the choice of biphenylic derivatives suitable for deracemization studies.

6. Experimental

6.1. Material and methods

Chemicals (Aldrich, Merck or Fluka) were of the highest grade available and were used without further purification. Solvents employed in the spectroscopic studies were of spectroscopic grade and used as received.

HPLC separation of the enantiomers of **2** was carried out on a Chiralpak AD column (250×4.6 mm i.d.). For the dynamic HPLC experiments, the column was placed inside a chromatographic oven with the temperature controlled within ±0.2°C and placing a 50 cm long inlet capillary inside the oven to ensure thermal equilibration of the mobile phase. Isolation of the two enantiomers of **2** for CD racemization studies was carried out on the

Table 3. Rotational barriers of **2** as obtained by experimental and theoretical approaches

Source	Rotational barrier (kcal/mol)	Solvent, temperature
Dynamic HPLC	21.9±0.2	Hexane/isopropanol 95/5,[a] 24°C
Circular dichroism	21.8±0.1	MeOH/H_2O 5/1,[a] 9°C
B3LYP/6-31G(d)	21.18	Vacuum, 25°C
B3LYP/6-311+G(d,p)	21.16	Vacuum, 25°C
HF/6-31G(d)	24.66	Vacuum, 25°C
MP2/6-31G(d)//HF/6-31G(d)	21.39	Vacuum

[a] 0.1% of trifluoroacetic acid added.

same column cooled at 4°C (water/ice bath). Racemic **2** was dissolved in the eluent (about 1 mg/ml) and 0.5 ml of the solution injected via a 2 ml loop. The fractions containing the two enantiomers were collected at 0°C and the solvent removed at reduced pressure at the same temperature. The isolated enantiomers were stored at −20°C until they were needed for the CD racemization experiments.

^{1}H NMR spectra were recorded on a Bruker AC 300 P spectrometer, operating at 300.13 and 75.47 MHz for ^{1}H and ^{13}C, respectively, equipped with a sample tube thermostating apparatus. Signals were referenced with respect to TMS ($\delta = 0.000$ ppm), used as internal standard in $CDCl_3$.

Kinetic studies on **2** were performed by circular dichroism on a Jasco spectropolarimeter J-715, equipped with a thermostating apparatus, using quartz cells of 1 cm path length.

2-Carboxy-2′-methoxy-6-nitrobiphenyl **2** was obtained by hydrolysis of 2-carboxymethyl-2′-metoxy-6-nitrobiphenyl **3** according to a previously described procedure.[3] Purification by chromatography on silica gel (ethyl acetate/isopropanol = 98/2) yielded a yellow solid (98%, melting point found 194–196°C).

^{1}H NMR δ ($CDCl_3$) ppm: 3.703 (s, 3H, OCH_3); 6.915 (d, 1H, 3′, $J_o = 8.2$ Hz, $J_m = 0.9$ Hz); 6.981 (t, 1H, 5′, $J_o = 7.3$ Hz, $J_m = 0.9$ Hz); 7.074 (d, 1H, 6′, $J_o = 7.3$ Hz, $J_m = 1.8$ Hz); 7.374 (m, 1H, 4′, $J_o = 8.2$ Hz; $J_o = 7.3$ Hz; $J_m = 1.8$ Hz); 7.562 (t, 1H, 4, $J_o = 7.9$ Hz); 7.965 (d, 1H, 5, $J_m = 1.2$ Hz, $J_o = 7.9$ Hz); 8.101 (d, 1H, 3, $J_m = 1.2$ Hz, $J_o = 7.9$ Hz). ^{13}C NMR δ ($CDCl_3$): 55.52; 110.81; 120.92; 123.69; 127.03; 128.20; 129.16; 130.33; 132.90; 133.10; 133.56; 151.25; 156.19; 169.72 ppm. Anal. calcd for $C_{14}H_{11}NO_5$: C, 61.54; H, 4.06; N, 5.13. Found: C, 61.04; H, 4.06; N, 5.05%.

2-Carboxymethyl-2′-metoxy-6-nitrobiphenyl **3** was prepared by an Ullman type arylic coupling reaction between 2-bromo-3-nitromethylbenzoate and 2-iodoanisole, according to a previously described procedure,[3] the ratio between the two reactants being 1:6. Purification of the obtained reddish oil by chromatography on silica gel (hexane/ether = 70/30) gave the desired product, a yellow solid (melting point found 90–92°C), in a 17% yield. ^{1}H NMR δ ($CDCl_3$) ppm: 3.584 (s, 3H, $OC\underline{H}_3$);3.714 (s, 3H, $COOC\underline{H}_3$); 6.928 (d, 1H, 3′, $J_o =$ 8.4 Hz, $J_m = 0.9$ Hz); 6.988 (t, 1H, 5′, $J_o = 7.3$ Hz, $J_m = 0.9$ Hz); 7.068 (d, 1H, 6′, $J_o = 7.3$ Hz, $J_m = 2.0$ Hz); 7.368 (m, 1H, 4′, $J_o = 8.4$ Hz, $J_o = 7.3$ Hz, $J_m = 2.0$ Hz); 7.539 (t, 1H, 4, $J_o = 8.1$ Hz, $J_o = 7.8$ Hz); 7.951 (d, 1H, 5, $J_o = 8.1$ Hz, $J_m = 1.4$ Hz); 8.008 (d, 1H, 3, $J_o = 7.8$ Hz, $J_m = 1.4$ Hz) ppm.

References

1. Belogi, G.; Croce, M.; Mancini, G. *Langmuir* **1997**, *13*, 2903–2904.
2. Borocci, S.; Erba, M.; Mancini, G.; Scipioni, A. *Langmuir* **1998**, *14*, 1960–1962.
3. Borocci, S.; Ceccacci, F.; Galantini, L.; Mancini, G.; Monti, D.; Scipioni, A.; Venanzi, M. *Chirality* **2003**, *15*, 441–447.
4. Nakagawa, H.; Kobori, Y.; Yoshida, M.; Yamada, K. *Chem. Commun.* **2001**, 2692–2693 and references cited therein.
5. Tobler, E.; Lammerhofer, M.; Mancini, G.; Lindner, W. *Chirality* **2001**, *13*, 641–647.
6. Li, C. C.; Adams, R. *J. Am. Chem. Soc.* **1935**, *57*, 1565–1569.
7. Trapp, O.; Schoetz, G.; Schurig, V. *Chirality* **2001**, *13*, 403–414.
8. Gasparrini, F.; Misiti, D.; Pierini, M.; Villani, C. *Tetrahedron: Asymmetry* **1997**, *8*, 2069–2073.
9. Maskill, H. *The Physical Basis of Organic Chemistry*; Oxford University Press: New York, 1998; pp. 280–282.
10. Biedermann, P. U.; Schurig, V.; Agranat, I. *Chirality* **1997**, *9*, 350–353.
11. Bortolotti, L. J.; Flurchick, K. In *Reviews in Computational Chemistry*; Lipkowitz, K. B.; Boyd, D. B., Eds.; VCH: New York, 1996; Vol. 7, Chapter 4.
12. (a) Grein, F. *J. Phys. Chem. A* **2002**, *106*, 3823–3827; (b) Arulmozhiraja, S.; Selvin, P. C.; Fujii, T. *J. Phys. Chem. A* **2002**, *106*, 1765–1769; (c) Arulmozhiraja, S.; Fujii, T. *J. Chem. Phys.* **2001**, *115*, 10589–10594.
13. Frisch, M. J.; Trucks, G. W.; Schlegel, H. B.; Scuseria, G. E.; Robb, M. A.; Cheeseman, J. R.; Zakrzewski, V. G.; Montgomery, J. A., Jr.; Stratmann, R. E.; Burant, J. C.; Dapprich, S.; Millam, J. M.; Daniels, A. D.; Kudin, K. N.; Strain, M. C.; Farkas, O.; Tomasi, J.; Barone, V.; Cossi, M.; Cammi, R.; Mennucci, B.; Pomelli, C.; Adamo, C.; Clifford, S.; Ochterski, J.; Petersson, G. A.; Ayala, P. Y.; Cui, Q.; Morokuma, K.; Malick, D. K.; Rabuck, A. D.; Raghavachari, K.; Foresman, J. B.; Cioslowski, J.; Ortiz, J. V.; Baboul, A. G.; Stefanov, B. B.; Liu, G.; Liashenko, A.; Piskorz, P.; Komaromi, I.; Gomperts, R.; Martin, R. L.; Fox, D. J.; Keith, T.; Al-Laham, M. A.; Peng, C. Y.; Nanayakkara, A.; Gonzalez, C.; Challacombe, M.; Gill, P. M. W.; Johnson, B.; Chen, W.; Wong, M. W.; Andres, J. L.; Gonzalez, C.; Head-Gordon, M.; Replogle, E. S.; and Pople, J. A. Gaussian 98, Revision A.7, Gaussian, Inc., Pittsburgh PA, 1998.
14. Schaftenaar, G.; Noordik, J. H. *J. Comput.-Aided Mol. Design* **2000**, *14*, 123–134.